Fault reactivation, leakage potential, and hydrocarbon column heights in the northern North Sea

David Wiprut and Mark D. Zoback

To investigate the question of how faults affect the migration of fluids in petroleum reservoirs, we evaluated the state of stress and pore pressure acting on the major faults in four oil and gas fields in the northern North Sea. Many of the faults bound hydrocarbon reservoirs. Our goal was to test the hypothesis that faults that are being reactivated in the current stress field are permeable and thus tend to leak, whereas those that are not (i.e. faults that are inactive in the current stress field) are likely to seal. To address this question, we utilize a detailed analysis of the magnitude and orientation of all three principal stresses in a number of wells in each field. These data, along with information on pore pressure, allowed us to resolve the shear and effective normal stress acting on distinct ~100 m × 100 m elements of individual fault planes. By comparing the stress state resolved on each fault element to expected stress at failure (using a Coulomb failure criterion) we created color-shaded maps showing the proximity to fault slip (and hence leakage) along each fault. Fault reactivation and hydrocarbon leakage in this area appears to be caused by three factors: (1) locally elevated pore pressure due to buoyant hydrocarbons in reservoirs abutting the faults, (2) fault orientations that are nearly optimally oriented for frictional slip in the present-day stress field, and (3) a relatively recent perturbation of the compressional stress caused by postglacial rebound. We demonstrate that the combination of these three factors may have recently induced fault slippage and gas leakage along sections of previously sealing reservoir-bounding faults in some fields, whereas in others, the stress and pore pressure are not sufficient to cause fault reactivation. We show that only in cases where reservoir-bounding faults are not potentially active, the pore-pressure difference across faults can become quite high. Hence, the leakage potential of reservoir-bounding faults appears to exert an important influence on potential hydrocarbon column heights.

Introduction

The question of how faults affect the migration of fluid in petroleum reservoirs is complicated, as some faults contribute dramatically to formation permeability (Dholakia et al., 1998) and allow hydrocarbon migration between different reservoir units (Finkbeiner et al., 2001), yet others provide effective barriers separating distinct reservoir compartments (Hunt, 1990). The sealing potential of a fault can be related to the juxtaposed lithologies across the fault and the presence or absence of seals resulting from the structure and content of the fault zone (Weber et al., 1978; Downey, 1984; Allan, 1989; Nybakken, 1991; Knipe, 1992; Berg and Avery, 1995; Fristad et al., 1997). However, the process by which a previously sealing fault begins to leak is unclear.

In this paper we consider the effect of fault reactivation on fault seal and fluid flow in the context of in-situ stress and pore pressure. We test the hypothesis that faults that are critically stressed in the current stress field (i.e. capable of slipping) are permeable, whereas those that are not critically stressed are not permeable. A number of permeability studies in fractured and faulted crystalline rock appear to confirm this hypothesis (Barton et al., 1995, 1998; Hickman et al., 1998; Townend and Zoback, 2000). Studies in hydrocarbon reservoirs in sedimentary basins in the Santa Maria Basin (Finkbeiner et al., 1997), the Gulf of Mexico (Finkbeiner et al., 2001), the Timor Sea (Castillo et al., 2000), and on a single partially leaking fault in the northern North Sea (Wiprut and Zoback, 2000b) appear to confirm that critically stressed faults are responsible for promoting hydrocarbon leakage and migration.

In this study we expand upon the work presented by Wiprut and Zoback (2000b) in the Visund field. The point of departure from our previous work is that we evaluate here the leakage potential of seismically mapped faults throughout the Visund field as well as three other fields in the northern North Sea (Fig. 1). We also address the effect of critically stressed faults and water-phase pore pressure on the potential height of hydrocarbon columns.

Hydrocarbon Seal Quantification edited by A.G. Koestler and R. Hunsdale. NPF Special Publication 11, pp. 203–219, Published by Elsevier Science B.V., Amsterdam.

surface (Byerlee, 1978). Fig. 3B shows a graphical representation of the preceding calculation. A fault element is plotted as a point within the 3-D Mohr circle according to the shear and normal stress resolved on the fault element. The slope of the Coulomb frictional failure line passing through the fault element point uniquely defines the critical pore pressure where the failure line intersects the normal-stress axis. The critical pore pressure is compared to a reference pore pressure line drawn through the data, where the pore-pressure data are combined across the entire field into a single one-dimensional model that varies with depth. The difference between the critical pore pressure and the reference pore pressure is called the critical pressure perturbation. This value shows how close the fault element is to slipping given the reference pore pressure determined for the field, and hence is a measure of the leakage potential.

The Visund field

The Visund field is located offshore Norway in the easternmost major fault block of the Tampen Spur (Færseth et al., 1995) along the western edge of the Viking graben. The reservoir is divided into several oil and gas compartments, some of which are separated by the A-Central fault (Fig. 4). Hydrocarbon columns were detected in the Brent group, which is the primary reservoir, as well as in the Statfjord and Amundsen formations. As shown in Fig. 4A, low seismic reflectivity along the southern part of the A-Central fault at the top Brent reservoir horizon is interpreted to be the result of gas leakage from the reservoir. The data in this region are of very high quality and there are no changes in lithology that might account for the change in seismic reflectivity. Fig. 4A also shows the mean orientation of the maximum horizontal stress determined in five wells in and near the Visund field from observations of drilling-induced tensile wall fractures (Moos and Zoback, 1990; Brudy and Zoback, 1993, 1999). Drilling-induced tensile wall fractures have been shown to be reliable indicators of the direction of the maximum horizontal stress (Brudy et al., 1997; Wiprut and Zoback, 2000a).

Fig. 4B shows a contour map of the top Brent reservoir horizon (red lines), with the faults, lateral extent of gas leakage (dashed line, see Fig. 4A), and outline of the map area shown in Fig. 4A (blue rectangle) superimposed on the structural contours. Exploration wells that yielded stress and pore-pressure data are shown with black circles. The Brent reservoir consists of a ridge running northeast–southwest with a saddle crossing perpendicular to the ridge between wells B and C. Comparison of the maps in Fig. 4A,B shows that the ridge is trapping gas along most of its length except for the portion of the ridge defined by the dashed low-reflectivity area. In the lower part of Fig. 4B, the southern boundary of the Brent reservoir plunges steeply into the Viking graben. This is the result of a large northeast–southwest trending graben-bounding fault that intersects the southern end of the A-Central fault. The effect of the graben-bounding fault can be seen in Fig. 4A as well, where there is a sharp transition from high to low reflectivity in the southern portion of the map.

Fig. 4C shows a schematic cross-section running approximately east–west through well D and the A-Central fault. The A-Central fault developed during the Jurassic as a normal fault with an ~60° dip (Færseth et al., 1995) and as much as 300 m of normal throw (L. Arnesen, pers. commun.). Since that time, the fault appears to have rotated and now dips between 30° and 45°. As a result, the A-Central fault is well oriented for being reactivated in a reverse sense in the current stress field. The other major faults in Visund generally dip 20° to 40° to the east, with some smaller antithetic faults dipping to the west.

Fig. 5 shows two views of the A-Central fault as determined from three-dimensional seismic reflection data. In the upper part of Fig. 5, a simplified map view of the fault is shown along with the orientation of the maximum horizontal stress in the three wells closest to the fault. The shaded area shows the lateral extent of gas leakage (simplified from Fig. 4A). In the lower part of Fig. 5, a perspective view of the approximately east-dipping fault surface is shown. A dark circle on the fault plane indicates the point where well D penetrates the A-Central fault. The fault plane is colored to indicate the leakage potential based on the orientation of the fault, the stress, and the pore pressure.

Fig. 6 shows a summary of the in-situ stress and pore-pressure data in the Visund field over the depth range of principal interest for the A-Central fault. The pore-pressure data are direct measurements made in the reservoir. The vertical stress was derived by using the average overburden gradient across the field. We calculated the overburden in each well by integrating density logs. The data for the minimum horizontal stress were derived from analysis of carefully conducted leak-off tests (LOTs). The magnitude of the maximum horizontal principal stress was determined from analysis of drilling-induced tensile fractures (following Zoback et al., 1993; Brudy et al., 1997). Determinations of stress magnitude and orientation in Visund are described in detail by Wiprut and Zoback (2000a).

The evidence for gas leakage in the immediate vicinity of the A-Central fault points to the fault as the possible conduit by which hydrocarbons are

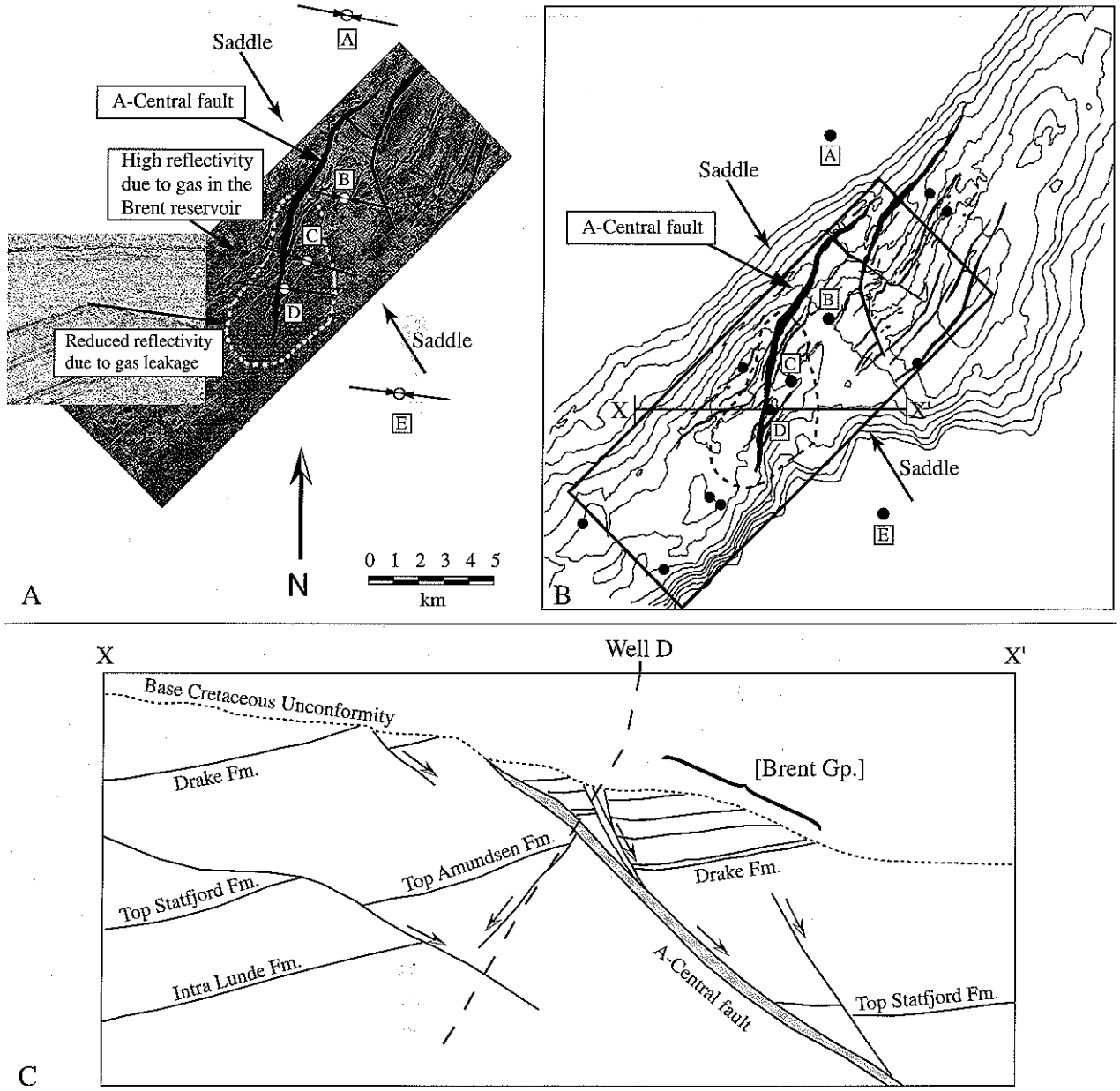

Fig. 4. (A) Map view of the Visund field showing seismic reflectivity of the reservoir horizon as well as the mean orientation of the maximum horizontal stress in five wells (A–E) (after Wiprut and Zoback, 2000b). (B) Contour map of the top Brent reservoir horizon. The saddle defines a local structural low along a ridge running from the northeast to the southwest. The area shown in part A is outlined in blue. (C) East–west cross-section along X–X′ (shown in part B) through the Visund field. Cap rock is defined by the short-dashed line at the base Cretaceous unconformity. The trajectory of well D through the A-Central fault is shown with long dashes.

escaping from the reservoir. We utilize the stress and pore-pressure trends shown in Fig. 6 to create the map of leakage potential shown in Fig. 5. The color shows the difference between the critical pore pressure we calculate and the reference pore-pressure line shown in Fig. 6. This difference is the critical pressure perturbation (defined previously). Hot colors indicate that a small increase in pore pressure ($<\sim$7 MPa) is enough to bring the fault to failure. Cool colors indicate that the pore pressure must rise significantly (>20 MPa) before those parts of the fault will begin to slip in the current stress field. Note that the largest part of the fault that is most likely to slip (indicated by the white outline) is located along the same part of the fault where leakage seems to be occurring. Note also that this portion of the fault is coincident with a change in the fault plane strike. Thus, there appears to be a qualitative correlation between the critically stressed fault criterion and the places along the fault where leakage appears to be occurring.

Well D was deviated to penetrate the A-Central fault at 2933 m true vertical depth (Fig. 5; horizontal dashed line, Fig. 6 inset), whereas wells B and C were drilled vertically. Because well D penetrates the

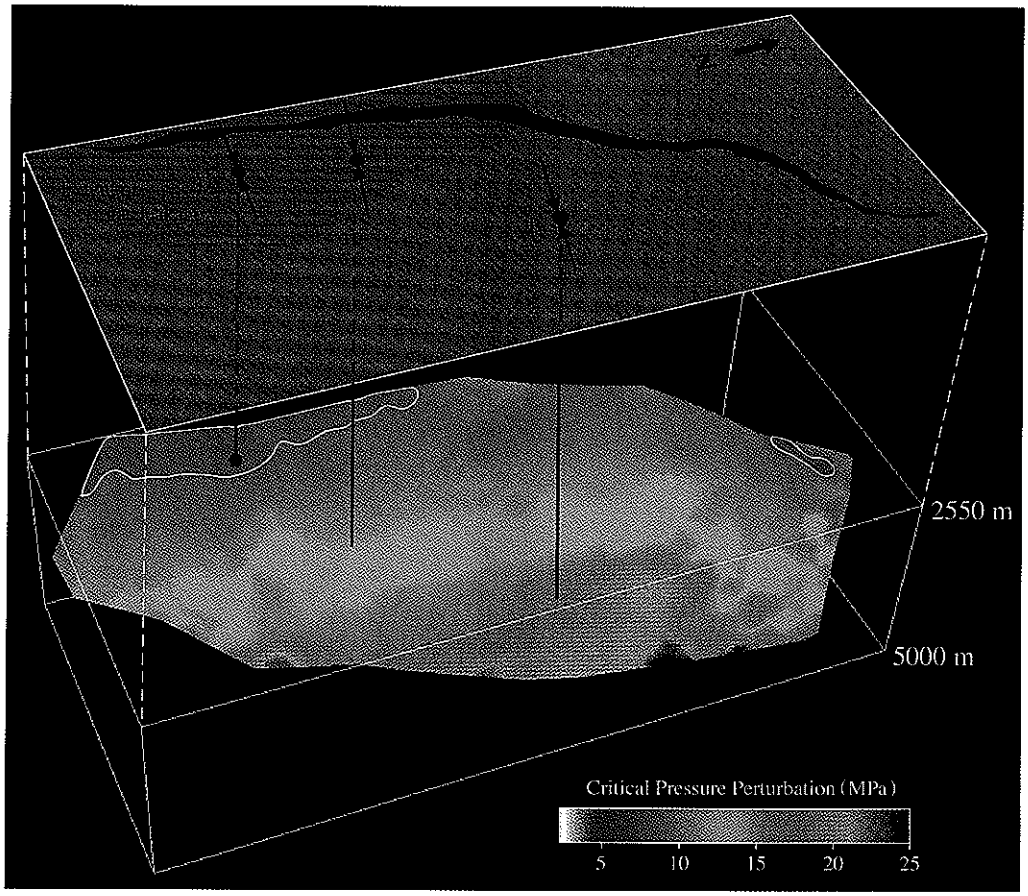

Fig. 5. Map view and perspective view of the A-Central fault as determined from a three-dimensional seismic reflection survey. Map view shows the region of gas leakage inferred from reduced seismic reflectivity (Fig. 4A). Perspective view is colored to show excess pore pressure (critical pressure perturbation) needed to induce fault slip in the current stress field. The white contours indicate portions of the fault that require an excess pore pressure less than approximately 7 MPa above the reference pore pressure. The largest part of the fault that is most likely to slip corresponds to that which appears to be leaking.

fault in this area, we can evaluate the correlation between the gas leakage and our prediction of leakage more quantitatively. Pore pressures in Visund are significantly above hydrostatic throughout the reservoir (Fig. 6). The inset of Fig. 6 shows a detailed view of the pore-pressure measurements in the three wells closest to the A-Central fault. The steep pressure gradient in well D is the result of light oil rather than free gas. A free gas cap was not detected in well D or well C, consistent with the reduced seismic reflectivity shown in Fig. 4A. As shown in the inset of Fig. 6, the pressure below the fault (indicated by the position of the dashed horizontal line) is within ~1 MPa of the theoretical critical pore pressure for fault slippage (the thick dashed line). This value is several megapascals above the reference pore pressure, just as predicted in Fig. 5.

Above the fault, pore pressures are significantly reduced, indicating that there is poor pressure communication across the fault (Fig. 6, inset). The A-Central fault is connected at its southern end with the graben-bounding fault described previously, preventing hydrocarbons from migrating around the southern end of the fault from the footwall to the hangingwall. Geochemical analysis of gas from both sides of the fault indicates that the hydrocarbons are derived from different sources (i.e. no fluid flow across the fault). Hydrocarbons are filling the reservoir on the eastern side of the A-Central fault from the east, and are filling the reservoir on the western side of the A-Central fault from the west (A. Wilhelms, pers. commun.).

It is interesting to note that although the pore pressure in the footwall appears to have caused the A-Central to slip and leak, both the footwall and hangingwall show reduced seismic reflectivity. Increased permeability resulting from fault slip seems to influence pore-pressure compartments on both sides of the fault. In this case, as with cases reported by Hickman et al. (1998) and Finkbeiner et al. (2001), fault slip appears to have principally promoted fault-parallel flow.

The pore pressures shown in the inset of Fig. 6 indicate that wells B, C and D are in approximately the same pressure compartment in the hangingwall, yet well B does not penetrate an area of reduced reflectivity. This is the result of the saddle shown in Fig. 4B.

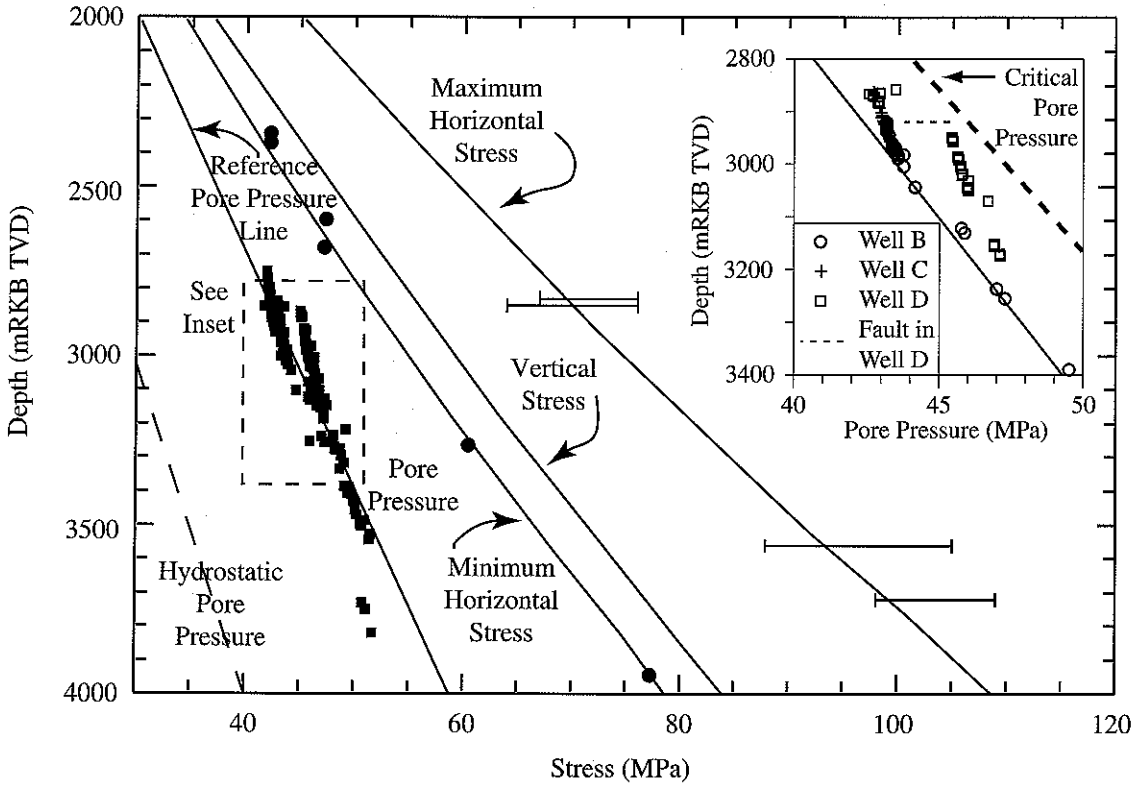

Fig. 6. In-situ stress and pore-pressure data obtained from wells throughout the Visund field. Best-fit lines to data are shown. Inset shows pore-pressure measurements in three wells drilled close to the A-Central fault.

The local structural low provided by the saddle effectively separates the hydrocarbon column in well B from wells C and D. There is an approximately 22-m difference in oil–water contacts between wells B and C; and there is an approximately 18-m gas column in well B that is absent in well C. Assuming the hydrocarbon columns were approximately the same before the fault leaked, the missing gas column in well C nearly accounts for the difference in oil–water contacts between the two wells.

Fig. 7 shows a perspective view, looking down and toward the north, of all the major faults in the Visund field with colors indicating the potential for hydrocarbon leakage. The perspective view in this figure creates distortions, therefore the scales are approximate. The five wells that provided data for the maximum horizontal stress are labeled, and other wells that provided pore-pressure data are shown as white circles. The faults are colored to indicate the likelihood of leakage along the surfaces. The leakage map indicates the potential for hydrocarbon leakage along any fault, and does not imply that any fault with red colors is currently leaking. A reservoir must abut the fault in the proper place, there must be hydrocarbons present to leak and the pore pressure must be high enough to reactivate the fault in order for the leakage to take place. The limits of this analysis are discussed in further detail below.

Fields 1, 2 and 3, northern North Sea

Fig. 8 shows the states of stress observed in Fields 1, 2 and 3, which we also studied in the northern North Sea. The general pore-pressure trend in Field 1 follows a nearly hydrostatic gradient until 3500 m, where it increases significantly in wells A, B and C (Fig. 8A). There is a marked pore-pressure difference between wells A and B, drilled into the hangingwall block of a major north–south trending and eastward dipping fault in Field 1, and well C drilled into the footwall block. Pore pressures in wells A and B follow a steep gas gradient toward the top of the hydrocarbon column, whereas the pore pressures in well C appear to primarily mirror the hydrostatic gradient at the same depth. The pore pressure in well C in a reservoir at greater depth follows a hydrocarbon gradient. The pore-pressure difference across the fault between wells B and C at a depth of 3450 m is shown by the arrow and is approximately 15 MPa. We discuss this large pore-pressure difference subsequently.

Pore pressures in both Field 2 and Field 3 are hydrostatic until approximately 3400 m, where there is an increase in pore pressure in both fields (Fig. 8B,C). The reservoir is highly overpressured in Field 3, and in Field 2 there is only moderate overpressure in the reservoir. The pore-pressure trends in both

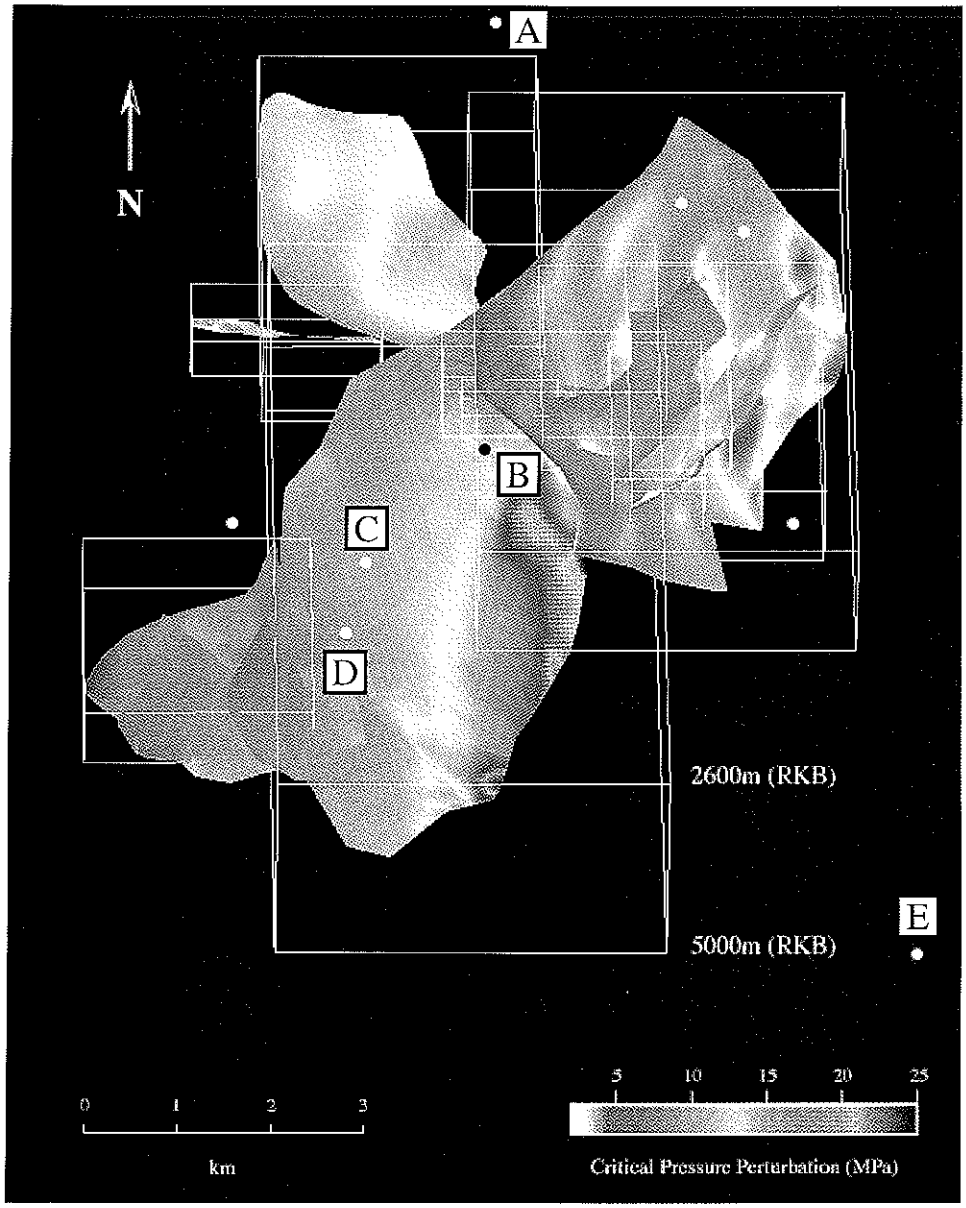

Fig. 7. Perspective view of fault surfaces in the Visund field showing leakage potential. The A-Central fault is shown with depths listed on the bounding box. Perspective view is colored to show excess pore pressure needed to induce fault slip in the current stress field. Hot colors indicate that the fault is close to failure and cool colors indicate that pore pressure must rise significantly (nearly 25 MPa) before fault will be reactivated in current stress field. Note that the scales are approximate, as the perspective view creates distortions.

fields continue to mirror the hydrostatic gradient in the overpressured sections. A number of anomalous pore-pressure measurements in the shallower parts of Field 2 (Fig. 8B) come from approximately five wells scattered throughout the region, and do not reflect the overall pore-pressure trend in any one compartment.

Note that in all three fields the maximum horizontal stress is distinctly larger than the vertical stress, and the minimum horizontal stress is close in magnitude to the vertical stress. This result is consistent with the strike-slip and reverse stress field indicated by earthquake focal-plane mechanisms (at 5 to 30 km depth) in this part of the North Sea (Lindholm et al., 1995).

Fig. 9A shows a map view of Fields 1 and 2 with the faults and mean orientation of the maximum horizontal stress determined in five wells in this area. Other exploration wells that yielded stress and pore-pressure data are shown by black circles. Field 1 is a small discovery approximately 5 km west of Field 2. Reservoirs in Field 1 are quite deep with Brent reservoir sandstones encountered between approximately 3500 and 4100 m. Structural dips are to the east between approximately 1° and 10° in Field 1 and between 2° and 14° in Field 2. Fig. 9B shows a schematic cross-section through well F in Field 2 that gives a generalized picture of the structure in this area. Major reservoir-bounding faults in this area

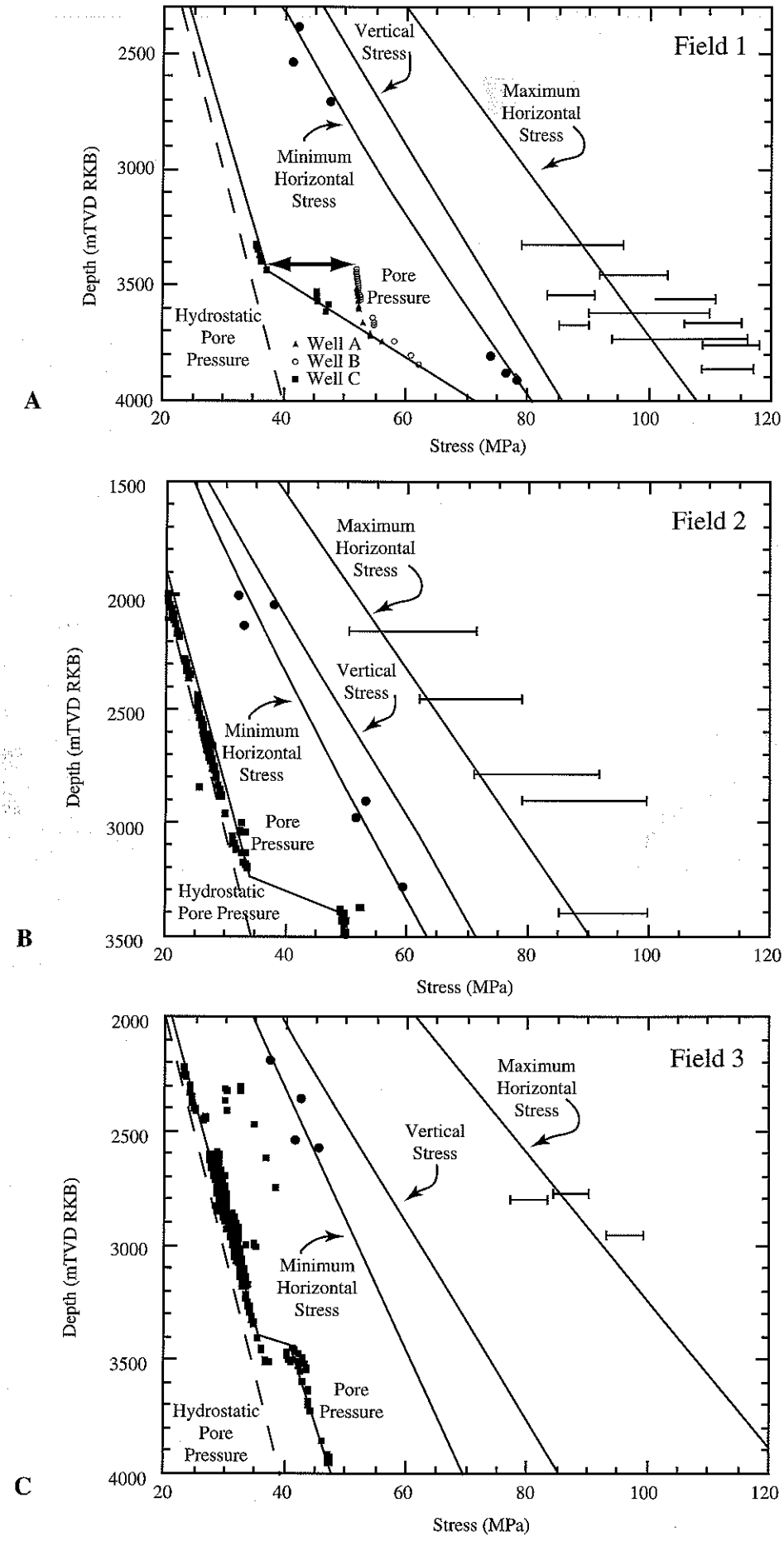

Fig. 8. In-situ stress and pore-pressure data obtained from wells throughout Field 1 (A), Field 2 (B), and Field 3 (C). Best-fit lines to data are shown. See text for explanation of arrow in (A).

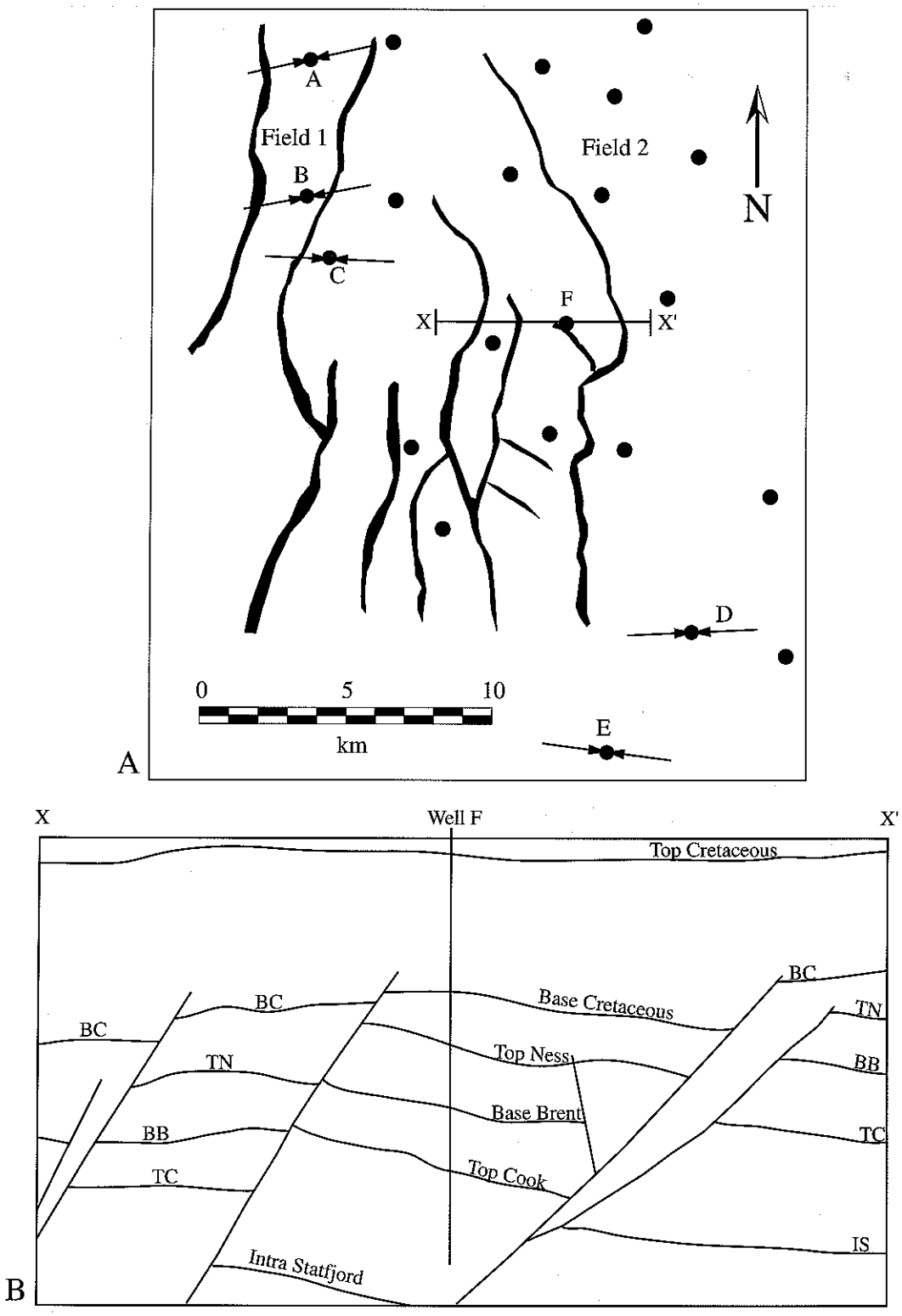

Fig. 9. (A) Generalized map of Field 1 and Field 2 showing the orientation of the maximum horizontal stress (inward pointed arrows), exploration wells (circles), and major faults. (B) East–west cross-section along X–X′ passing through well F in Field 2. Major faults generally dip steeply west toward the Viking graben.

strike approximately north–south, and dip to the west between 40° and 55°. Careful examination of seismic cross-sections in Field 1 and Field 2 revealed no evidence of hydrocarbon leakage, and there is no evidence of hydrocarbon migration at present in these fields. Field 1 and Field 2 are highly compartmentalized by faults.

Fig. 10 shows a perspective view of all the major faults in Fields 1 and 2 with colors indicating the potential for hydrocarbon leakage as in Figs. 5 and 7.

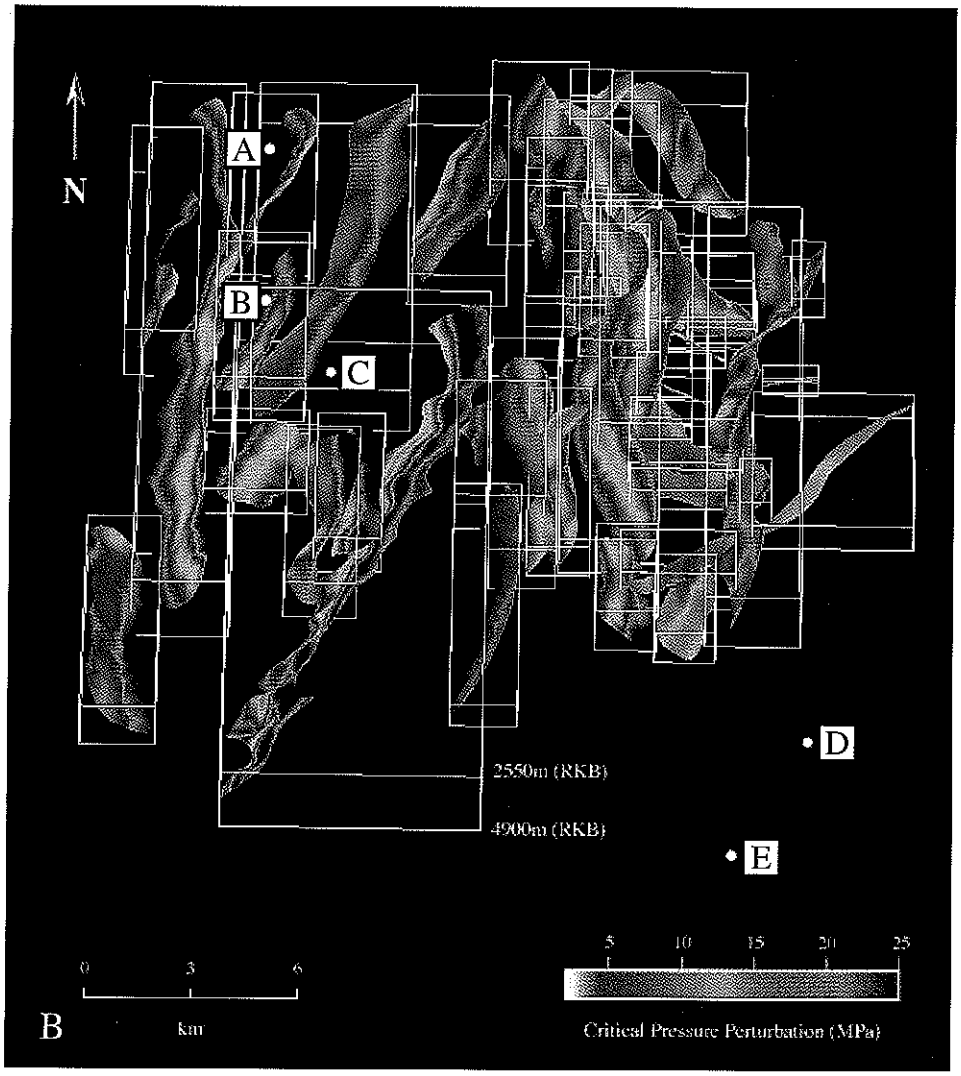

Fig. 10. Fault leakage potential in Field 1 and Field 2. See Fig. 7 for explanation.

The five wells that provided data for the maximum horizontal stress are labeled. Note that most of the faults in Fields 1 and 2 do not show any significant potential for leakage. This is primarily the result of the faults being poorly oriented for frictional failure in the current stress field. This prediction is consistent with the absence of hydrocarbon leakage and migration in these fields. Fig. 10 shows that our analysis predicts there should be no leakage and it also shows that the reservoirs may potentially maintain large pore-pressure differences across compartments. According to our analysis, the major fault to the east of well B in Field 1 can potentially maintain up to approximately 15 to 17 MPa pore-pressure difference across its surface at the weakest points. As noted above, the pore-pressure data in this field show a pressure difference of approximately 15 MPa between the pore-pressure trend used to create Fig. 10 and the hydrocarbon column supported by the major fault east of well B (Fig. 8A, see arrow).

Fig. 11A shows a map view of Field 3 with the faults and mean orientation of the maximum horizontal stress determined in four wells in this area. Other exploration wells that yielded stress and pore-pressure data are shown with black circles. Fig. 11B shows a schematic cross-section through two wells in the field along the line W–W′. The Brent reservoir in Field 3 typically dips between 3° and 10° to the east and southeast in individual fault blocks, but overall becomes shallower to the south-southeast in this region. Reservoir-bounding faults in Field 3 generally strike in two directions, with a northeast–southwest striking set of faults cross-cutting a north–south striking set. The faults typically dip between 50° and 60° throughout the field. Fig. 12 shows three east–west oriented cross-sections cut through wells A and F along the lines X–X′, Y–Y′, and Z–Z′ shown in Fig. 11. Cross-section Y–Y′ indicates that there is some amplitude dimming above the fault east of well A, which is interpreted to be the result of gas

those that are not critically stressed are more likely to be sealing. Fault reactivation and hydrocarbon leakage in this area appear to be caused by three factors: (1) locally elevated pore pressure due to buoyant hydrocarbons abutting faults, (2) fault orientations that are nearly optimally oriented for frictional slip in the present-day stress field, and (3) a recent perturbation of the compressional stress associated with postglacial rebound. The combination of these three factors may have recently induced fault slippage and gas leakage along sections of previously sealing reservoir-bounding faults in some fields, whereas in others, the stress and pore pressure are not sufficient to cause fault reactivation. In cases where reservoir-bounding faults are not potentially active, the pore-pressure difference across faults can become quite high. Hence, the leakage potential of reservoir-bounding faults appears to exert an important influence on potential hydrocarbon column heights.

Acknowledgements

We thank Norsk Hydro for providing the data and financial support for this project. We thank Bjorn Larsen for suggesting that this work be initiated at Norsk Hydro. We also thank Linn Arnesen, Nils Kageson-Loe, Roald Færseth, Arnd Wilhelms, and Paul Gillespie at Norsk Hydro for their efforts to provide us with data and for helpful discussions.

References

Allan, U.S., 1989. Model for hydrocarbon migration and entrapment within faulted structures. Bull. Am. Assoc. Pet. Geol., 73: 803–811.

Barton, C.A., Zoback, M.D. and Moos, D., 1995. Fluid flow along potentially active faults in crystalline rock. Geology, 23: 683–686.

Barton, C.A., Hickman, S.H., Morin, R., Zoback, M.D. and Benoit, D., 1998. Reservoir-scale fracture permeability in the Dixie Valley, Nevada, geothermal field. In: Proceedings of SPE/ISRM Rock Mechanics in Petroleum Engineering, Trondheim, 2. Society of Petroleum Engineers, pp. 315–322.

Berg, R.R. and Avery, A.H., 1995. Sealing properties of Tertiary growth faults, Texas Gulf Coast. Am. Assoc. Pet. Geol. Bull., 79: 375–393.

Brudy, M. and Zoback, M.D., 1993. Compressive and tensile failure of boreholes arbitrarily-inclined to principal stress axes: application to the KTB boreholes, Germany. Int. J. Rock Mech. Min. Sci. Geomech. Abstr., 30: 1035–1038.

Brudy, M. and Zoback, M.D., 1999. Drilling-induced tensile wall-fractures: implications for determination of in-situ stress orientation and magnitude. Int. J. Rock Mech. Min. Sci., 36: 191–215.

Brudy, M., Zoback, M.D., Fuchs, K., Rummel, F. and Baumgärtner, J., 1997. Estimation of the complete stress tensor to 8 km depth in the KTB scientific drill holes: Implications for crustal strength. J. Geophys. Res., 102: 18453–18475.

Byerlee, J.D., 1978. Friction of rocks. Pure Appl. Geophys., 116: 615–629.

Castillo, D.A., Bishop, D.J., Donaldson, I., Kuek, D., de Ruig, M., Trupp, M. and Shuster, M.W., 2000. Trap integrity in the Laminaria High–Nancar Trough region, Timor Sea: prediction of fault seal failure using well-constrained stress tensors and fault surfaces interpreted from 3D seismic. Aust. Pet. Produc. Explor. Assoc. J., 40, part 1: 151–173.

Dholakia, S.K., Aydin, A., Pollard, D.D. and Zoback, M.D., 1998. Fault-controlled hydrocarbon pathways in the Monterey Formation, California. Am. Assoc. Pet. Geol. Bull., 82 (8): 1551–1574.

Doré, A.G. and Lundin, E.R., 1996. Cenozoic compressional structures on the NE Atlantic margin: nature, origin and potential significance for hydrocarbon exploration. Pet. Geosci., 2: 299–311.

Downey, M.W., 1984. Evaluating seals for hydrocarbon accumulations. Am. Assoc. Pet. Geol. Bull., 68: 1752–1763.

Finkbeiner, T., Barton, C. and Zoback, M.D., 1997. Relationships among in-situ stress, fractures and faults, and fluid flow; Monterey Formation, Santa Maria Basin, California. Am. Assoc. Pet. Geol. Bull., 81 (12): 1975–1999.

Finkbeiner, T., Zoback, M.D., Flemings, P. and Stump, B., 2001. Stress, pore pressure, and dynamically constrained hydrocarbon columns in the South Eugene Island 330 Field, northern Gulf of Mexico. Am. Assoc. Pet. Geol. Bull., 85(6): 1007–1031.

Færseth, R.B., Sjøblom, T.S., Steel, R.J., Liljedahl, T., Sauar, B.E. and Tjelland, T., 1995. Tectonic controls on Bathonian–Volgian syn-rift successions on the Visund fault block, northern North Sea. In: R.J. Steel, V. Felt, E.P. Johannessen and C. Mathieu (Editors), Sequence Stratigraphy of the Northwest European Margin. Norwegian Petroleum Society (NPF), Special Publication 5. Elsevier, Amsterdam, pp. 325–346.

Fristad, T., Groth, A., Yielding, G. and Freeman, B., 1997. Quantitative fault seal prediction — a case study from Oseberg Syd. In: P. Møller-Pedersen and A.G. Koestler (Editors), Hydrocarbon Seals: Importance for Exploration and Production. Norwegian Petroleum Society (NPF), Special Publication 7. Elsevier, Amsterdam, pp. 107–125.

Grollimund, B., 2000. Impact of Deglaciation on Stress and Implications for Seismicity and Hydrocarbon Exploration. Ph.D. dissertation, Stanford University.

Grollimund, B. and Zoback, M.D., 2000. Post glacial lithospheric flexure and induced stresses and pore pressure changes in the northern North Sea. Tectonophysics, 327: 61–81.

Hermanrud, C., Norgård Bolås, H.M., Mari, H., Fichler, C., Romes, A. and Heggland, R., 1997. Studies of hydrocarbon migration; an important discipline in hydrocarbon exploration. Am. Assoc. Pet. Geol. Bull., 81: 1383.

Hickman, S.H., Zoback, M.D. and Benoit, R., 1998. Tectonic controls on fault-zone permeability in a geothermal reservoir at Dixie Valley, Nevada. In: Proceedings of SPE/ISRM Rock Mechanics in Petroleum Engineering, Trondheim, 1. Society of Petroleum Engineers, pp. 79–86.

Hunt, J.M., 1990. Generation and migration of petroleum from abnormally pressured fluid compartments. Am. Assoc. Pet. Geol. Bull., 74: 1–12.

Jaeger, J.C. and Cook, N.G.W., 1979. Fundamentals of Rock Mechanics (3rd ed.). Chapman and Hall, New York, 593 pp.

Klemann, V. and Wolf, D., 1998. Modeling of stresses in the Fennoscandian lithosphere induced by Pleistocene glaciations. Tectonophysics, 294: 291–303.

Knipe, R.J., 1992. Faulting processes and fault seal. In: R.M. Larsen, H. Brekke, B.T. Larsen and E. Talleraas (Editors), Structural and Tectonic Modelling and its Application to Petroleum Geology. Norwegian Petroleum Society (NPF), Special Publication 1. Elsevier, Amsterdam, pp. 325–342.

Law, B.E. and Spencer, C.W., 1998. Abnormal pressure in hydrocarbon environments. Am. Assoc. Pet. Geol. Mem., 70: 1–11.

Lindholm, C.D., Bungum, H., Villagran, M. and Hicks, E., 1995. Crustal stress and tectonics in Norwegian regions determined from earthquake focal mechanisms. In: Proceedings of the Workshop on Rock Stresses in the North Sea, Trondheim, Feb. 13–14. SINTEF Rock and Mineral Engineering, pp. 77–91.

Moos, D. and Zoback, M.D., 1990. Utilization of observations of well bore failure to constrain the orientation and magnitude of crustal stresses: Application to continental, Deep Sea Drilling Project, and Ocean Drilling Program boreholes. J. Geophys. Res., 95: 9305–9325.

Nybakken, S., 1991. Sealing fault traps — an exploration concept in a mature petroleum province: Tampen Spur, northern North Sea. First Break, 9: 209–222.

Rohrman, M., van der Beek, P., Andriessen, P. and Cloetingh, S., 1995. Meso–Cenozoic morphotectonic evolution of southern Norway: Neogene domal uplift inferred from apatite fission track thermochronology. Tectonics, 14 (3): 704–718.

Sibson, R.H., 1992. Implications of fault-valve behaviour for rupture nucleation and recurrence. In: T. Mikumo, K. Aki, M. Ohnaka, L.J. Ruff and P.K.P. Spudich (Editors), Earthqake Source Physics and Earthquake Precursors. Tectonophysics, 211: 283–293.

Stephansson, O., 1988. Ridge push and glacial rebound as rock stress generators in Fennoscandia. Bull. Geol. Inst. Univ. Uppsala, N.S., 14: 39–48.

Townend, J. and Zoback, M.D., 2000. How faulting keeps the crust strong. Geology, 28: 399–402.

Vågnes, E., Gabrielsen, R.H. and Haremo, P., 1998. Late Cretaceous–Cenozoic intraplate contractional deformation at the Norwegian continental shelf: timing, magnitude and regional implications. Tectonophysics, 300: 29–46.

Weber, K.J., Mandl, G., Pilaar, W.F., Lehner, F. and Precious, R.G., 1978. The role of faults in hydrocarbon migration and trapping in Nigerian growth fault structures. Offshore Technology Conference, 10, Paper OTC 3356, pp. 2643–2653.

Wiprut, D.J. and Zoback, M.D., 2000a. Constraining the full stress tensor in the Visund field, Norwegian North Sea: application to wellbore stability and sand production. Int. J. Rock Mech. Min. Sci., 37: 317–336.

Wiprut, D. and Zoback, M.D., 2000b. Fault reactivation and fluid flow along a previously dormant normal fault in the northern North Sea. Geology, 28 (7): 595–598.

Zoback, M.D., Apel, R., Baumgärtner, J., Brudy, M., Emmermann, R., Engeser, B., Fuchs, K., Kessel, W., Rischmüller, H., Rummel, F. and Vernik, L., 1993. Upper crustal strength inferred from stress measurements to 6 km depth in the KTB borehole. Nature, 365: 633–635.

D. WIPRUT *Department of Geophysics, 397 Panama Mall, Stanford University, Stanford, CA 94305-2215, USA*
Present address: GeoMechanics International Inc., Parmelia House Level 1, 191 St. George's Terrace, Perth, WA 6000, Australia. E-mail: wiprut@geomi.com

M.D. ZOBACK *Department of Geophysics, 397 Panama Mall, Stanford University, Stanford, CA 94305-2215, USA*